

AD-A071 390 OKLAHOMA UNIV NORMAN SCHOOL OF AEROSPACE MECHANICAL --ETC F/G 11/4  
FINITE-ELEMENT ANALYSIS OF LAMINATED COMPOSITE-MATERIAL PLATES.(U)  
JUN 79 J N REDDY N00014-78-C-0647

UNCLASSIFIED

OU-AMNE-79-9

NL

| OF |  
AD  
A071390



END  
DATE  
FILMED  
9-79  
DDC



MICROCOPY RESOLUTION TEST CHART  
NATIONAL BUREAU OF STANDARDS-1963-A

# LEVEL

12

ADA071390

Department of the Navy  
OFFICE OF NAVAL RESEARCH  
Structural Mechanics Program  
Arlington, Virginia 22217

Contract N00014-78-C-0647  
Project NR 064-609  
Technical Report No. 3

Report OU-AMNE-79-9

### FINITE-ELEMENT ANALYSES OF LAMINATED COMPOSITE-MATERIAL PLATES

*See 1473 in back*

by

J. N. Reddy

June 1979

DDC  
RECEIVED  
JUL 19 1979  
D

DDC FILE COPY

Accession For	
NTIS GRA&I	<input checked="" type="checkbox"/>
DDC TAB	<input type="checkbox"/>
Unannounced	<input type="checkbox"/>
Justification	<input type="checkbox"/>
By _____	
Distribution/	
Availability/	
Dist	Avail and/or special
A	

School of Aerospace, Mechanical and Nuclear Engineering  
University of Oklahoma  
Norman, Oklahoma 73019

Approved for public release; distribution unlimited

79 07 17 023

# FINITE-ELEMENT ANALYSIS OF LAMINATED COMPOSITE-MATERIAL PLATES

J. N. Reddy

School of Aerospace, Mechanical and Nuclear Engineering  
The University of Oklahoma, Norman, OK 73019

## SUMMARY

A finite-element formulation of the equations governing the laminated anisotropic plate theory of Yang, Norris and Stavsky is presented. The theory is a generalization of Mindlin's theory for isotropic plates to laminated anisotropic plates and includes shear deformation and rotary inertia effects. Finite-element solutions are presented for rectangular plates of antisymmetric angle-ply laminates having material properties that are typical of a highly anisotropic composite material. Two sets of material properties that are typical of advanced fiber-reinforced composites are used to show the parametric effects of plate aspect ratio, length-to-thickness ratio, number of layers, and lamination angle. The element is also employed to study the bending of laminated, anisotropic bimodulus-material plates. Results are presented for single-layer and two-layer cross-ply rectangular plates subjected to sinusoidal loading.

The report also presents a  $C^0$  finite element for the von Karman equations of thin elastic plates. The slope-displacement relations are treated as constraints using the so-called penalty method of Courant. The resulting element contains the transverse deflection and two slopes as nodal degrees of freedom. By selecting an appropriate value of the penalty parameter, solutions for thin as well as thick plates are obtained. Numerical results are presented for rectangular plates with various edge conditions.

## 1. INTRODUCTION

The classical thin-plate theory assumes that normals to the midsurface before deformation remain straight and normal to the midsurface after deformation, implying that the transverse shear deformations are negligible. As a result the free vibration frequencies calculated using the thin-plate theory are higher than those obtained by the Mindlin plate theory [1], which includes transverse shear flexibility and rotary inertia effects; the deviation increases with increasing mode number. The transverse shear effects are even more pronounced, due to the low transverse shear moduli relative to the in-plane Young's moduli, in the case of filamentary composite plates. A reliable prediction of the response characteristics of high-modulus composite plates requires the use of shear deformable theory.

A number of shear deformable theories have been proposed to date. The first such theory for laminated isotropic plates is apparently due to Stavsky [2]. The theory has been generalized to laminated anisotropic plates by Yang, Norris and Stavsky [3]. A good review of various other theories (e.g., [4,5]) can be found in [6]. It has been shown (see, for example, [5-8]) that the Yang-Norris-Stavsky (YNS) theory is adequate for predicting the flexural vibration response of laminated anisotropic plates in the first few modes. Whitney and Pagano [9] applied the YNS theory to the cylindrical bending of antisymmetric cross-ply and angle-ply plate strips under sinusoidal loading and free vibration of antisymmetric angle-ply plate strips (see also [10,11]). More recently, Bert and Chen [12] presented, using the YNS theory, a closed-form solution for the free vibration of simply supported rectangular plates of antisymmetric angle-ply laminates.

While considerable effort has been expended in the finite-element vibration analysis of isotropic plates, only limited investigations of laminated

anisotropic plates can be found in the literature [13-16]. Exploiting the symmetries exhibited by anisotropic plates, Noor and Mathers [13,14] studied the effects of shear deformation and anisotropy on the accuracy and convergence of several shear-flexible displacement finite-element models based on a form of Reissner's plate theory. The analysis was limited to symmetrically laminated cross-ply plates. In [15,16] vibration of only cross-ply laminated plates was considered.

All of the plate bending elements based on the displacement type formulations are algebraically complex (require  $C^1$ -continuity; see Kawai and Yoshimura [22]) and are computationally too expensive to use in nonlinear analyses. Several  $C^0$  elements have been developed in the last decade in the interest of computational efficiency in large nonlinear problems. These include the so-called mixed finite elements (see, Hermann [23], Nemat-Nasser and Lee [24], Kikuchi and Ando [25], and Reddy and Tsay [26]), and elements based on the discrete "Kirchhoff hypothesis" of Wempner, Oden and Kross [27] and Fried [28], and on the "reduced integration" techniques of Fried [29], Zienkiewicz and Hinton [30], and Hughes, Cohen, and Haroun [31]. In these works only linear plate bending problems were considered.

The purpose of the present investigation is two-fold: to develop a finite-element model based on Yang-Norris-Stavsky (YNS) theory, and to present a penalty-finite element that treats the slope-displacement relations as constraints. The relationship between the penalty formulation and Reissner-Mindlin thick-plate equations is established. Numerical results are presented for free vibration of antisymmetric, angle-ply laminated-composite plates (based on YNS theory), and for nonlinear bending (based on von Karman theory) of thin plates. Results are compared with the closed-form and other approximate solutions.

Following this introduction, we review the equations of the Yang-Morris-Stavsky theory, and present an associated variational formulation, which is required for the finite-element modeling.

## 2. GOVERNING EQUATIONS AND VARIATIONAL FORMULATION

Consider a plate of constant thickness  $h$  composed of an even number of thin anisotropic layers oriented alternately at angles  $\theta$  and  $-\theta$ . The origin of the coordinate system is located at the middle plane of the plate with the  $z$ -axis being normal to the mid-plane. The material of each layer is assumed to possess a plane of elastic symmetry parallel to the  $xy$ -plane. We shall denote the middle plane with  $\Omega$ .

The YNS theory is based on the following assumed displacement field:

$$\begin{aligned} u &= u_0(x, y, \bar{t}) + z \psi_x(x, y, \bar{t}) \\ v &= v_0(x, y, \bar{t}) + z \psi_y(x, y, \bar{t}) \\ w &= w(x, y, \bar{t}) \end{aligned} \quad (1)$$

where  $u$ ,  $v$ , and  $w$  are the displacement components in the  $x$ ,  $y$  and  $z$ -directions, respectively,  $u_0$  and  $v_0$  are the in-plane (stretching) displacements of the middle plane, and  $\psi_x$  and  $\psi_y$  are the shear rotations. Recalling the strain-displacement equations of linear elasticity, we have

$$\begin{aligned} \epsilon_x &= \frac{\partial u_0}{\partial x} + z \frac{\partial \psi_x}{\partial x}, & \epsilon_y &= \frac{\partial v_0}{\partial y} + z \frac{\partial \psi_y}{\partial y}, & \epsilon_z &= 0 \\ \gamma_{xy} &= \frac{\partial u_0}{\partial y} + \frac{\partial v_0}{\partial x} + z \left( \frac{\partial \psi_x}{\partial y} + \frac{\partial \psi_y}{\partial x} \right), \\ \gamma_{xz} &= \psi_x + \frac{\partial w}{\partial x}, & \gamma_{yz} &= \psi_y + \frac{\partial w}{\partial y} \end{aligned} \quad (2)$$

Owing to the existence of a plane of elastic symmetry, the constitutive relations for any layer in the  $(x,y)$  system are given by

$$\begin{bmatrix} \sigma_x \\ \sigma_y \\ \tau_{yz} \\ \tau_{xz} \\ \tau_{xy} \end{bmatrix} = \begin{bmatrix} Q_{11} & Q_{12} & 0 & 0 & Q_{16} \\ Q_{12} & Q_{22} & 0 & 0 & Q_{26} \\ 0 & 0 & Q_{44} & Q_{45} & 0 \\ 0 & 0 & Q_{45} & Q_{55} & 0 \\ Q_{16} & Q_{26} & 0 & 0 & Q_{66} \end{bmatrix} \begin{bmatrix} \epsilon_x \\ \epsilon_y \\ \gamma_{yz} \\ \gamma_{xz} \\ \gamma_{xy} \end{bmatrix} \quad (3)$$

where  $Q_{ij}$  are the plane-stress reduced stiffness components of the layer material.

Introducing the stress and moment resultants per unit length,

$$\begin{aligned} (N_1, N_2, N_6) &= \int_{-t/2}^{t/2} (\sigma_x, \sigma_y, \tau_{xy}) dz, & (Q_x, Q_y) &= \int_{-t/2}^{t/2} (\tau_{xz}, \tau_{yz}) dz \\ (M_1, M_2, M_6) &= \int_{-t/2}^{t/2} (\sigma_x, \sigma_y, \tau_{xy}) z dz \end{aligned} \quad (4)$$

we can write (2) and (3) in terms of the resultants and displacements:

$$\begin{bmatrix} N_1 \\ N_2 \\ Q_y \\ Q_x \\ N_6 \\ M_1 \\ M_2 \\ M_6 \end{bmatrix} = \begin{bmatrix} A_{11} & A_{12} & 0 & 0 & A_{16} & B_{11} & B_{12} & B_{16} \\ A_{12} & A_{22} & 0 & 0 & A_{26} & B_{12} & B_{22} & B_{26} \\ 0 & 0 & A_{44} & A_{45} & 0 & 0 & 0 & 0 \\ 0 & 0 & A_{45} & A_{55} & 0 & 0 & 0 & 0 \\ A_{16} & A_{26} & 0 & 0 & A_{66} & B_{16} & B_{26} & B_{66} \\ B_{11} & B_{12} & 0 & 0 & B_{16} & D_{11} & D_{12} & D_{16} \\ B_{12} & B_{22} & 0 & 0 & B_{26} & D_{12} & D_{22} & D_{26} \\ B_{16} & B_{26} & 0 & 0 & B_{66} & D_{16} & D_{26} & D_{66} \end{bmatrix} \begin{bmatrix} \frac{\partial u_0}{\partial x} \\ \frac{\partial v_0}{\partial y} \\ \frac{\partial w}{\partial y} + \psi_y \\ \frac{\partial w}{\partial x} + \psi_x \\ \frac{\partial u_0}{\partial y} + \frac{\partial v_0}{\partial x} \\ \frac{\partial \psi}{\partial x} \\ \frac{\partial \psi}{\partial y} \\ \frac{\partial \psi}{\partial y} + \frac{\partial \psi}{\partial x} \end{bmatrix} \quad (5)$$

The laminate stiffnesses  $A_{ij}$ ,  $B_{ij}$ , and  $D_{ij}$  are given by

$$(A_{ij}, B_{ij}, D_{ij}) = \int_{-t/2}^{t/2} Q_{ij}^{(m)}(1, z, z^2) dz, \quad (i, j = 1, 2, 6) \quad (6)$$

$$A_{ij} = k_{ij} \int_{-t/2}^{t/2} Q_{ij}^{(m)} dz \quad (i, j = 4, 5),$$

The stiffness coefficients  $Q_{ij}^{(m)}$  depend on the material properties and orientation of the  $m$ -th layer. The parameters  $k_{ij}$  are the shear correction coefficients. Note that for antisymmetric laminates, coefficients  $A_{16}$ ,  $A_{26}$ ,  $A_{45}$ ,  $B_{11}$ ,  $B_{12}$ ,  $B_{22}$ ,  $D_{16}$ , and  $D_{26}$  are identically zero.

In the absence of body forces, the equations of motion associated with the YNS theory are (see [3]),

$$\frac{\partial N_1}{\partial x} + \frac{\partial N_6}{\partial y} = p \frac{\partial^2 u}{\partial \bar{t}^2}$$

$$\frac{\partial N_6}{\partial x} + \frac{\partial N_2}{\partial y} = p \frac{\partial^2 v}{\partial \bar{t}^2}$$

$$\frac{\partial Q_x}{\partial x} + \frac{\partial Q_y}{\partial y} = p \frac{\partial^2 w}{\partial \bar{t}^2} \quad (7)$$

$$\frac{\partial M_1}{\partial x} + \frac{\partial M_6}{\partial y} - Q_x = I \frac{\partial^2 \psi_x}{\partial \bar{t}^2}$$

$$\frac{\partial M_6}{\partial x} + \frac{\partial M_2}{\partial y} - Q_y = I \frac{\partial^2 \psi_y}{\partial \bar{t}^2}$$

where  $p$  and  $I$  are the normal and rotary inertia coefficients,

$$(p, I) = \int_{-t/2}^{t/2} (1, z^2) \rho dz \quad (8)$$

$\rho$  being the material density of the plate (made of identical layers).

With the finite-element discretization in mind, we give a variational form of the equations in (7). The kinetic energy and the strain energy associated with the problem are,

$$T = \frac{1}{2} \int_{\Omega} \left\{ \rho \left[ \left( \frac{\partial u}{\partial t} \right)^2 + \left( \frac{\partial v}{\partial t} \right)^2 + \left( \frac{\partial w}{\partial t} \right)^2 \right] + I \left[ \left( \frac{\partial \psi}{\partial t} \right)^2 + \left( \frac{\partial \phi}{\partial t} \right)^2 \right] \right\} dA d\bar{t} \quad (9)$$

$$U = \frac{1}{2} \int_{\Omega} \int_{-t/2}^{t/2} \sigma_{ij} \epsilon_{ij} dA dz ,$$

Using equations (2) and (4), one can express the strain energy in terms of the displacements and the slope functions as

$$\begin{aligned} U = & \frac{1}{2} \int_{\Omega} \left\{ A_{11} \left( \frac{\partial u_0}{\partial x} \right)^2 + 2A_{16} \frac{\partial u_0}{\partial x} \frac{\partial u_0}{\partial y} + A_{66} \left( \frac{\partial u_0}{\partial y} \right)^2 + \frac{\partial u_0}{\partial x} \left( A_{12} \frac{\partial v_0}{\partial y} + A_{16} \frac{\partial v_0}{\partial x} \right) \right. \\ & + \frac{\partial v_0}{\partial y} \left( A_{12} \frac{\partial u_0}{\partial x} + A_{26} \frac{\partial u_0}{\partial y} \right) + \frac{\partial v_0}{\partial y} \left( A_{26} \frac{\partial v_0}{\partial y} + A_{66} \frac{\partial v_0}{\partial x} \right) \\ & + \frac{\partial v_0}{\partial x} \left( A_{16} \frac{\partial u_0}{\partial x} + A_{66} \frac{\partial u_0}{\partial y} \right) + A_{22} \left( \frac{\partial v_0}{\partial y} \right)^2 + 2A_{26} \frac{\partial v_0}{\partial y} \frac{\partial v_0}{\partial x} \\ & + A_{66} \left( \frac{\partial v_0}{\partial x} \right)^2 + \frac{\partial u_0}{\partial x} \left( B_{11} \frac{\partial \psi}{\partial x} + B_{16} \frac{\partial \psi}{\partial y} + B_{12} \frac{\partial \phi}{\partial y} + B_{16} \frac{\partial \phi}{\partial x} \right) \\ & + \left( \frac{\partial u_0}{\partial y} + \frac{\partial v_0}{\partial x} \right) \left( B_{16} \frac{\partial \psi}{\partial x} + B_{66} \frac{\partial \psi}{\partial y} + B_{26} \frac{\partial \phi}{\partial y} + B_{66} \frac{\partial \phi}{\partial x} \right) \\ & + \frac{\partial v_0}{\partial y} \left( B_{12} \frac{\partial \psi}{\partial x} + B_{26} \frac{\partial \psi}{\partial y} + B_{22} \frac{\partial \phi}{\partial y} + B_{26} \frac{\partial \phi}{\partial x} \right) + \frac{\partial \psi}{\partial x} \left( B_{11} \frac{\partial u_0}{\partial x} \right. \\ & + B_{16} \frac{\partial u_0}{\partial y} + B_{12} \frac{\partial v_0}{\partial y} + B_{16} \frac{\partial v_0}{\partial x} \left. \right) + \left( \frac{\partial \psi}{\partial y} + \frac{\partial \phi}{\partial x} \right) \left( B_{16} \frac{\partial u_0}{\partial x} + B_{66} \frac{\partial u_0}{\partial y} \right. \\ & + B_{26} \frac{\partial v_0}{\partial y} + B_{66} \frac{\partial v_0}{\partial x} \left. \right) + \frac{\partial \phi}{\partial y} \left( B_{12} \frac{\partial u_0}{\partial x} + B_{26} \frac{\partial u_0}{\partial y} + B_{22} \frac{\partial v_0}{\partial y} \right. \\ & + B_{26} \frac{\partial v_0}{\partial x} \left. \right) + A_{44} \left( \frac{\partial w}{\partial y} \right)^2 + 2A_{45} \frac{\partial w}{\partial x} \frac{\partial w}{\partial y} + A_{55} \left( \frac{\partial w}{\partial x} \right)^2 \\ & + \frac{\partial w}{\partial y} \left( A_{44} \psi_y + A_{45} \psi_x \right) + \frac{\partial w}{\partial x} \left( A_{45} \psi_y + A_{55} \psi_x \right) \\ & + \psi_x \left( A_{45} \frac{\partial w}{\partial y} + A_{55} \frac{\partial w}{\partial x} \right) + \psi_y \left( A_{44} \frac{\partial w}{\partial y} + A_{45} \frac{\partial w}{\partial x} \right) \end{aligned}$$

$$\begin{aligned}
& + D_{11} \left( \frac{\partial \psi_x}{\partial x} \right)^2 + 2D_{16} \frac{\partial \psi_x}{\partial x} \frac{\partial \psi_x}{\partial y} + D_{66} \left( \frac{\partial \psi_x}{\partial y} \right)^2 + A_{55} \psi_x^2 \\
& + \frac{\partial \psi_x}{\partial x} \left( D_{12} \frac{\partial \psi_y}{\partial y} + 2D_{16} \frac{\partial \psi_y}{\partial x} \right) + \frac{\partial \psi_y}{\partial y} \left( D_{12} \frac{\partial \psi_x}{\partial x} + 2D_{26} \frac{\partial \psi_x}{\partial y} \right) \\
& + 2D_{66} \frac{\partial \psi_x}{\partial y} \frac{\partial \psi_y}{\partial x} + 2A_{45} \psi_x \psi_y + D_{22} \left( \frac{\partial \psi_y}{\partial y} \right)^2 + 2D_{26} \frac{\partial \psi_y}{\partial x} \frac{\partial \psi_y}{\partial y} \\
& + D_{66} \left( \frac{\partial \psi_y}{\partial x} \right)^2 + A_{44} \psi_y^2 \} dA
\end{aligned} \tag{10}$$

It can be verified that the first variation of the Lagrangian functional,  $L=T-V$  (i.e. Hamilton's principle) leads to the equations of motion (7) expressed in terms of the displacements and slope functions. Here  $V$  denotes the total potential energy (i.e. sum of the strain energy and energy due to applied loads) of the plate.

### 3. FINITE-ELEMENT MODELS OF THE YNS THEORY

The first variation of the Lagrangian functional,  $L = T-V$ , gives the variational form of the equations of motion governing the layered anisotropic plates. This variational form is convenient for the finite-element formulation. Since we are primarily interested here in the free vibration analysis, the potential energy due to the applied loads is zero.

Let the domain  $\Omega$  be decomposed into a set of finite elements. The restriction of the Lagrangian functional  $L$  to the finite element  $\Omega_e$  is denoted by  $L_e$ . We have

$$L = \sum_{e=1}^N L_e(u_0^e, v_0^e, w^e, \psi_x^e, \psi_y^e) \tag{11}$$

where  $N$  denotes the total number of finite elements in the mesh. Over each element  $\Omega_e$ , the field variables  $(u_0^e, v_0^e, w^e, \psi_x^e, \psi_y^e)$  can be represented by the following approximation

$$u_0^e = \sum_i^r u_i^e \phi_i, \quad v_0^e = \sum_i^r v_i^e \phi_i, \quad \text{etc.} \quad (12)$$

where  $\phi_i^e(x,y)$  are finite-element interpolation functions (also called shape functions). For simplicity, the same interpolation is employed for all of the five fields. Substitution of equation (12) into the first variation  $\delta L_e$  of  $L_e$  gives (omitting the algebraic details) the following set of equations for a typical element  $\Omega_e$ :

$$[M] \{\delta\} + [K] \{\Delta\} = \{0\} \quad (13)$$

where  $\{\Delta\} = \{ \{u_i\}^T, \{v_i\}^T, \{w_i\}^T, \{\psi_x^i\}^T, \{\psi_y^i\}^T \}^T$  is a  $5r$  by  $1$  column vector, and

$$[K] = \begin{bmatrix} [K^{11}] & [K^{12}] & [0] & [K^{14}] & [K^{15}] \\ & [K^{22}] & [0] & [K^{24}] & [K^{25}] \\ & & [K^{33}] & [K^{34}] & [K^{35}] \\ \text{symmetric} & & & [K^{44}] & [K^{45}] \\ & & & & [K^{55}] \end{bmatrix} \quad [M] = \begin{bmatrix} [M^1] & & & & \\ & [M^1] & & & \\ & & [M^1] & & \\ & & & [M^2] & \\ & & & & [M^2] \end{bmatrix}$$

The elements  $K_{ij}^{\alpha\beta}$  ( $\alpha, \beta = 1, 2, \dots, 5$ ;  $i, j = 1, 2, \dots, r$ ) of the stiffness matrix and  $M_{ij}^{\alpha}$  of the mass matrix are defined by

$$K_{ij}^{11} = A_{11} S_{ij}^x + A_{16} (S_{ij}^{xy} + S_{ji}^{xy}) + A_{66} S_{ij}^y$$

$$K_{ij}^{12} = A_{12} S_{ij}^{xy} + A_{16} S_{ij}^x + A_{26} S_{ij}^y + A_{66} S_{ji}^{xy}$$

$$K_{ij}^{14} = B_{11} S_{ij}^x + B_{16} (S_{ij}^{xy} + S_{ji}^{xy}) + B_{66} S_{ij}^y$$

$$K_{ij}^{15} = B_{12} S_{ij}^{xy} + B_{16} S_{ij}^x + B_{26} S_{ij}^y + B_{66} S_{ji}^{xy}$$

$$K_{ij}^{22} = A_{26} (S_{ij}^{xy} + S_{ji}^{xy}) + A_{22} S_{ij}^y + A_{66} S_{ij}^x$$

$$\begin{aligned}
K_{ij}^{24} &= B_{12} S_{ij}^{xy} + B_{16} S_{ij}^x + B_{26} S_{ij}^y + B_{66} S_{ij}^{xy} \\
K_{ij}^{25} &= B_{26} (S_{ij}^{xy} + S_{ji}^{xy}) + B_{66} S_{ij}^x + B_{22} S_{ij}^y \\
K_{ij}^{33} &= A_{55} S_{ij}^x + A_{44} S_{ij}^y, \quad K_{ij}^{34} = A_{55} S_{ij}^{ox}, \quad K_{ij}^{35} = A_{44} S_{ij}^{oy} \\
K_{ij}^{44} &= D_{11} S_{ij}^x + D_{16} (S_{ij}^{xy} + S_{ji}^{xy}) + D_{66} S_{ij}^y + A_{55} S_{ij} \\
K_{ij}^{45} &= D_{12} S_{ij}^{xy} + D_{66} S_{ji}^{xy} + D_{16} S_{ij}^x + D_{26} S_{ij}^y \\
K_{ij}^{55} &= D_{26} (S_{ij}^{xy} + S_{ji}^{xy}) + D_{66} S_{ij}^x + D_{22} S_{ij}^y + A_{44} S_{ij} \\
M_{ij}^1 &= \rho S_{ij}, \quad M_{ij}^2 = I S_{ij}
\end{aligned} \tag{14}$$

and,

$$S_{ij}^{\xi\eta} = \int_{D_e} \frac{\partial \phi_i}{\partial \xi} \frac{\partial \phi_j}{\partial \eta} dx dy, \quad S_{ij}^{00} = S_{ij}, \quad S_{ij}^{\xi\xi} = S_{ij}^{\xi} \tag{15}$$

Note that in the above derivation, the parameter  $A_{45}$  is set to zero for simplicity.

For free vibration, the (discrete) equations of motion (13), after assembly of the elements, take the form of a standard eigenvalue problem:

$$([K] - \omega^2 [M])\{\Delta\} = \{0\} \tag{16}$$

where  $\omega$  is the frequency of the natural vibration. Equation (16) can be solved, after imposing the boundary conditions of the problem, by any standard eigenvalue program.

Several comments are in order on the finite-element equations (16). In theory, each layer of the plate can have its own material properties and angle of orientation. The material properties of each layer are generally

known in its own coordinate system. Hence, they must be transformed, using the angle of orientation, to the plate coordinates (see [17]) to get  $Q_{ij}^{(m)}$  for each lamina. To obtain  $A_{ij}$ ,  $B_{ij}$ , and  $D_{ij}$  one must use equations (10). For example,

$$A_{ij} = \int_{-t/2}^{t/2} Q_{ij} dz = \sum_{m=1}^L \int_{Z_m}^{Z_{m+1}} Q_{ij}^{(m)} dz \quad (17)$$

where  $Z_m$  is the distance from the mid-plane, along the thickness, of the lower surface of the  $m$ th layer. Thus, once  $A_{ij}$ ,  $B_{ij}$  and  $D_{ij}$  are known for the layered composite plate, it can be viewed as a plate made of single material having behavior characterized by the constants  $A_{ij}$ ,  $B_{ij}$  and  $D_{ij}$ . Consequently, the finite element procedure becomes the one that is used in Mindlin's plate theory.

In the present study the eight-node ( $r=8$ ) rectangular elements (of the serendipity family) are used. The element stiffness matrix is of order 40 by 40.

#### 4. FREE VIBRATION ANALYSIS BASED ON THE YNS THEORY

Numerical results are presented for antisymmetric angle-ply rectangular plates with all four edges simply supported. All of the layers are assumed to be of the same thickness and made of the same orthotropic material. Hence, the coefficients  $Q_{ij}$  referred to the material-symmetry axes are given by

$$[Q'] = \begin{bmatrix} \alpha E_1 & \alpha \nu_{12} E_2 & 0 & 0 & 0 \\ \alpha \nu_{12} E_2 & \alpha E_2 & 0 & 0 & 0 \\ 0 & 0 & G_{12} & 0 & 0 \\ 0 & 0 & 0 & kG_{13} & 0 \\ 0 & 0 & 0 & 0 & kG_{23} \end{bmatrix}, \quad k = 5/6, \quad \alpha = (1 - \nu_{12}\nu_{21})^{-1}$$

In addition to the isotropic properties, the following two sets of dimensionless material properties (typical of two kinds of graphite-epoxy) are used:

1. Isotropic:  $E_1/E_2 = 1.0$  ,  $G_{12}/E_2 = 1/2(1+\nu)$  ,  $\nu = 0.3$
2. Material I:  $E_1/E_2 = 40$  ,  $G_{12}/E_2 = 0.6$  ,  $G_{13}/E_2 = G_{23}/E_2 = 0.5$  ,  $\nu_{12} = 0.25$
3. Material II:  $E_1/E_2 = 25$  ,  $G_{12}/E_2 = 0.5$  ,  $G_{13}/E_2 = 0.2$  ,  $\nu_{12} = 0.25$

All of the computations were carried out on an IBM 370/158 in double precision. Due to storage limitations, only a quarter plate (exploiting the biaxial

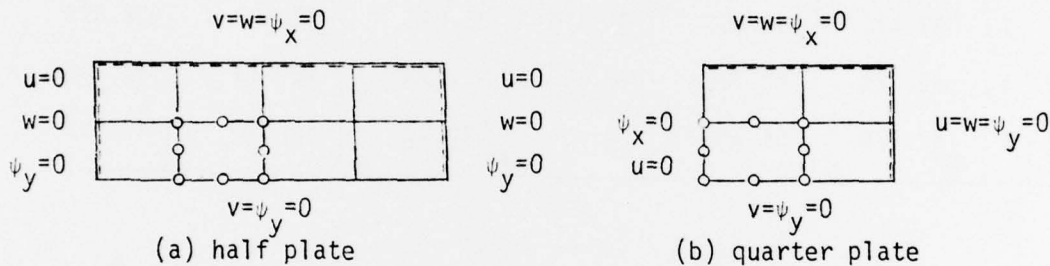


Figure 1 Boundary conditions and the finite element mesh for the simply supported plate.

symmetry) is used to compute the fundamental natural frequencies and a half-plate model is used to obtain the symmetric and antisymmetric higher order modes. The finite-element mesh and the boundary conditions for the simply supported edges are shown in Figure 1.

As a check for the numerical accuracy of the finite element method, natural frequencies were first obtained for a thick isotropic plate ( $\nu = 0.3$ ) with side-to-thickness ratio of 10. The finite-element results are compared with 3-D linear-elasticity solution, Mindlin's thick-plate theory, and the classical thin-plate theory in Table 1. The finite-element solution was obtained using 2x2 and 4x2 quadratic element meshes in the half plate. Clearly, the results obtained by using the 4x2 mesh are closer to the thick-plate theory indicating that further mesh refinements could yield better accuracy. However, with the increasing mode number, the finite-element results

Table 1 Comparison of nondimensional frequencies  $\lambda = \omega a^2 (\rho/Et^2)^{1/2}$   
of a square simply supported isotropic plate ( $\nu = 0.3$ ,  $a/t = 10$ )

m	n	3-D Linear Elasticity Solution [8]	Mindlin's Thick Plate Solution [18]	Rock and Hinton [19]	Present FEM Half Plate Model		Classical Plate Theory
					3 DOF(4x2)	5 DOF(2x2)	
1	1	5.780	5.767	5.774	5.793	5.920	5.973
1	2	13.805	13.755	13.749	14.081	15.251	14.934
1	3	25.867	25.700	27.207	27.545	28.133	29.867
2	3	32.491	32.230	34.010	35.040	33.057	38.829
3	3	42.724	42.302	48.609	49.693	49.723	53.868
1	5	57.476	56.758	—	74.823	74.041	77.652

Table 2 Effects of in-plane displacements, lamination angle, and the finite-element mesh on the dimensionless fundamental frequency,  $\lambda = \omega a^2 (\rho/E_2 t^2)^{1/2}$ , of a simply supported square plate ( $a/t = 10$ ,  $a/b = 1$ , 4 layers)

M a t e r i a l	$\theta$	0°		30°			45°		
		NDF=3	NDF=5	NDF=3	NDF=5	[12]	NDF=3	NDF=5	[12]
	Mesh								
I	1x1	14.504	16.8	18.492	19.268		19.412	20.183	
	2x2	14.193	14.193	18.229	17.689	17.63	19.154	18.609	18.46
II	1x1	10.539	11.978	13.164	13.543		13.738	13.993	
	2x2	10.358	10.358	13.013	12.739		13.591	13.303	

seem to deviate more from the 3-D elasticity and Mindlin's thick plate solutions.

Figure 2 shows a plot of the dimensionless frequency versus the side-to-thickness ratio for three aspect ratios of layered composite plate consisting of four Material I layers oriented at  $45^\circ/-45^\circ/45^\circ/-45^\circ$ . The results are compared with the closed-form solution of Bert and Chen [12]. For a given aspect ratio, the finite-element results seem to approach the closed-form solution with a decreasing side-to-thickness ratio. The figure also indicates that the finite-element solution converges to the exact with decreasing aspect ratio. Figure 2 also contains a plot of the fundamental frequency versus the side-to-thickness ratio of a square plate consisting of four layers of Material II. All of the results were obtained using a  $2 \times 2$  mesh of quadratic elements in the quarter plate.

Table 2 shows the effect of in-plane displacements, the lamination angle, and the mesh on the fundamental natural frequency of square laminated plates consisting of four layers ( $a/t = 10$ ). The three-degree-of-freedom (NDF = 3) solution is obtained by suppressing the inplane displacement degrees of freedom ( $u, v$ ). It is clear that the fundamental frequency increases with the lamination angle (results are symmetric with respect to  $45^\circ$ , i.e., results for  $90^\circ - \theta$  are identical to those of  $\theta$ ), and the 3-degree-of-freedom ( $w, \psi_x, \psi_y$ ) prediction results in higher frequencies. Due to storage limitation further refinement of the mesh was not possible; however, the finite-element solution seems to converge toward the closed-form solution.

The effects of the lamination angle and the number of layers on the dimensionless fundamental frequency are shown in Table 3. The finite element method predicts the lower values for the frequencies compared to the closed form solution of Bert and Chen [12] as the number of layers is increased.

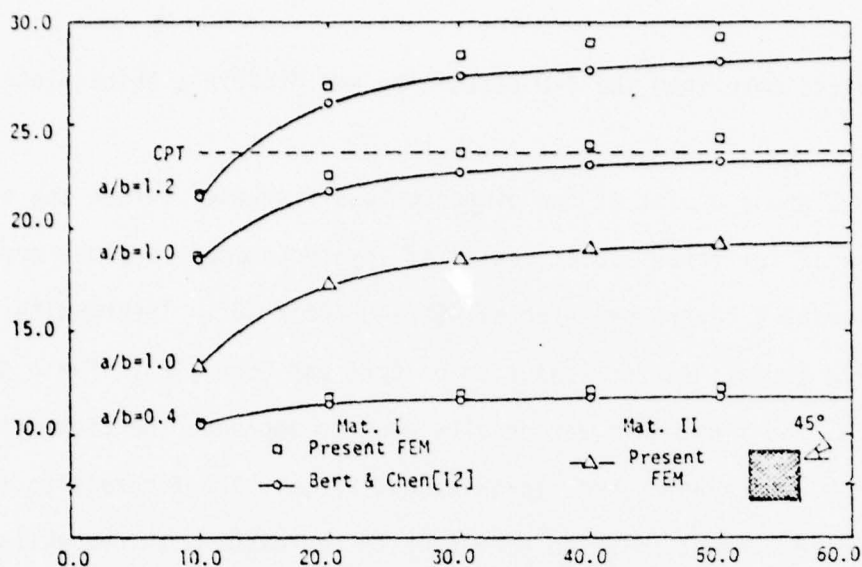


Figure 2 Comparison of fundamental frequency for a four-layer antisymmetric angle-ply ( $\theta=45^\circ$ ) simply supported square plate by classical plate theory (CPT) and shear deformation theory of Ref. [3].

Table 3 Effects of lamination angle ( $\theta$ ) and number of layers on the dimensionless fundamental frequency  $\omega a^2 (\rho/E_2 t^2)^{1/2}$  of a simply supported square plate ( $\theta/-\theta/\theta/.../-\theta$ ,  $a/t = 10$ )

No. of Layers	Material Type I				Material Type II	
	30°		45°		30°	45°
	Present*	[12]	Present*	[12]	Present*	
2	15.001	12.68	15.715	13.04	11.351	11.752
4	17.689	17.63	18.609	18.46	12.739	13.303
6	18.002	18.23	18.925	19.09	12.898	13.471
8	18.104	18.42	19.028	19.29	12.950	13.524
10	18.150	18.51	19.074	19.38	12.973	13.549
12	18.175	—	19.093	—	12.985	13.562
14	18.189	—	19.113	—	12.993	13.569
16	18.199	18.60	19.122	19.48	12.998	13.575

\* 2x2 quadratic element is used

Tables 4 and 5 show the effects of plate aspect ratio and length-to-thickness ratio on the dimensionless fundamental frequency (recall Figure 2) for Material I while Tables 6 and 7 contain similar results for Material II. The results are obtained using 2 by 2 mesh of quadratic elements. From Table 4, it is clear that the finite-element results are closer, but higher, than the closed-form solution of Reference [12].

Finally, Table 8 shows a comparison of nondimensional frequencies, for a four layered laminated square plate ( $45^\circ/-45^\circ/45^\circ/-45^\circ$ ,  $a/h = 10$ ), obtained by various investigators. The table includes the closed-form solution of Bert and Chen [12], classical plate theory [20], and the finite-element solutions obtained using various meshes and with and without in-plane displacement degrees of freedom (DOF). While the 4 by 2, 3-DOF model gives better results than the 2 by 2, 3 DOF model, the 2 by 2, 5-DOF model gives more accurate results when compared to the closed-form solution.

While the present study concentrated on the antisymmetric, angle-ply laminated plates with simply-supported edge conditions, the theory presented (and the computer program developed) is valid for general laminated plates, and for various other edge conditions (see Reddy [21]).

##### 5. PENALTY FORMULATION OF VON KARMAN PLATE EQUATIONS

Let the middle plane  $\Omega \subset \mathbb{R}^2$  of the plate coincide with the  $(x,y)$  plane, and let  $\partial\Omega$  be its piecewise smooth boundary. The strain-energy functional associated with the nonlinear (von Karman) theory of thin, isotropic plates is

$$U_c(w) = \frac{D}{2} \int_{\Omega} \left[ (w_{,xx})^2 + (w_{,yy})^2 + 2\nu w_{,xx} w_{,yy} + 2(1-\nu) (w_{,xy})^2 \right] dx dy + U_n(w, w_{,x}, w_{,y}) \quad (13)$$

where  $U_n(\cdot)$  is the contribution due to the large-deflection assumption,

Table 4 Effects of plate aspect ratio  $(a/b)$  and length-to-thickness ratio  $(a/t)$  on the dimensionless fundamental frequency,  $\lambda = \omega a^2 (\rho/E_2 t^2)^{1/2}$  of a simply-supported rectangular plate made of Material I ( $45^\circ/-45^\circ/45^\circ/-45^\circ$ ).

$a/b$ $a/t$	0.2	0.4	0.6	0.8	1.0	1.2	1.4	1.6	1.8	2.0
10	8.724* (8.664)	10.535 (10.42)	12.965 (12.82)	15.712 (15.54)	18.609 (18.46)	21.567 (21.51)	24.602 (24.67)	27.736 (27.95)	30.981	34.347 (34.87)
20	9.475 (9.300)	11.767 (11.46)	14.896 (14.45)	18.557 (17.97)	22.584 (21.87)	26.857 (26.12)	31.401 (30.68)	36.240 (35.56)	41.372	46.789 (46.26)
30	9.667 (9.436)	12.074 (11.70)	15.385 (14.84)	19.304 (18.56)	23.676 (22.74)	28.381 (27.35)	33.457 (32.38)	38.940 (37.82)	44.832	51.132 (49.98)
40	9.759 (9.485)	12.205 (11.78)	15.583 (14.98)	19.604 (18.78)	24.118 (23.08)	29.003 (27.83)	34.307 (33.05)	40.071 (38.72)	46.305	53.012 (51.52)
50	9.816 (9.507)	12.280 (11.82)	15.689 (15.04)	19.759 (18.89)	24.343 (23.24)	29.321 (28.06)	34.742 (33.37)	40.653 (39.17)	47.067	53.989 (52.29)

\* Values in brackets are from Ref. [12]

Table 5 Effects of plate aspect ratio ( $a/b$ ) and length-to-thickness ratio ( $a/t$ ) on the dimensionless fundamental frequency,  $\lambda = \omega a^2 (\rho/E_2 t^2)^{1/2}$ , of a simply-supported rectangular plate made of Material I ( $30^\circ/-30^\circ/30^\circ/-30^\circ$ ).

$a/b$ $a/t$	0.2	0.4	0.6	0.8	1.0	1.2	1.4	1.6	1.8	2.0
10	11.106	12.172	13.734	15.615	17.689	19.880	26.275	24.460	26.836	29.288
20	12.595	13.950	15.969	18.457	21.281	24.362	27.645	31.088	34.680	38.428
30	12.972	14.401	16.543	19.204	22.253	25.619	29.244	33.086	37.132	41.390
40	13.136	14.591	16.779	19.507	22.646	26.128	29.896	33.909	38.154	42.641
50	13.233	14.700	16.908	19.667	22.850	26.389	30.229	34.330	38.677	43.284
60	13.301	14.773	16.992	19.767	22.974	26.545	30.426	34.577	38.985	43.663

Table 7 Effects of plate aspect ratio ( $a/b$ ) and length-to-thickness ratio ( $a/t$ ) on the dimensionless fundamental frequency,  $\lambda = \omega a^2 (\rho/E_2 t^2)^{1/2}$ , of a simply-supported rectangular plate made of Material II ( $30^\circ/-30^\circ/30^\circ/-30^\circ$ ).

$a/b$ $a/t$	0.2	0.4	0.6	0.8	1.0	1.2	1.4	1.6	1.8	2.0
10	8.198	8.937	10.019	11.316	12.739	14.237	15.785	17.382	19.038	20.771
20	9.788	10.819	12.351	14.233	16.363	18.674	21.126	23.697	26.383	29.791
30	10.214	11.333	13.009	15.088	17.471	20.094	22.913	25.905	29.064	32.397
40	10.392	11.545	13.277	15.439	17.929	20.688	23.673	26.859	30.242	33.831
50	10.490	11.659	13.418	15.619	18.163	20.992	24.062	27.351	30.855	34.582
60	10.555	11.731	13.505	15.728	18.302	21.770	24.291	27.640	31.216	35.026

Table 6 Effects of plate aspect ratio (a/b) and length-to-thickness ratio (a/t) on the dimensionless fundamental frequency,  $\lambda = \omega a^2 (\rho/E_2 t)^{1/2}$ , of a simply-supported rectangular plate made of Material II (45°/-45°/45°/-45°)

a/b \ a/t	0.2	0.4	0.6	0.8	1.0	1.2	1.4	1.6	1.8	2.0
10	6.670	7.890	9.533	11.378	13.303	15.259	17.256	19.310	21.437	23.642
20	7.517	9.232	11.574	14.298	17.266	20.401	23.707	27.193	30.860	34.704
30	7.733	9.584	12.137	15.151	18.499	22.100	25.967	30.117	34.551	39.266
40	7.828	9.730	12.365	15.501	19.012	22.819	26.944	31.410	36.222	41.381
50	7.883	9.808	12.484	15.679	19.273	23.188	27.449	32.083	37.101	42.504
60	7.922	9.859	12.556	15.784	19.427	23.405	27.746	32.481	37.621	—

Table 8 Comparison of nondimensional frequencies  $\lambda = \omega a^2 (\rho/E_2 t^2)^{1/2}$ ,  
of a four-layer laminated simply supported plate  
(Material 1, 45 /-45 /45 /-45 ,  $a/t = 10$ )

m	n	Bert & Chen [12]	Present FEM (based on the YNS theory)				Classical Plate Theory
			Quarter plate 2x2, NDF=5	Half plate 2x2, NDF=5	Half plate 2x2, NDF=3	Half plate 4x2, NDF=3	
1	1	18.46	18.609	18.259	19.244	19.153	23.53
1	2	34.87	—	35.585	36.512	35.405	53.74
1	3	54.27	54.360	54.3675	55.727	55.390	98.87
2	3	67.17	—	70.315	70.895	67.637	147.65
1	4	75.58	—	79.315	79.882	76.412	160.35
3	3	82.84	83.975	99.5975	100.012	84.725	211.75
1	5	97.56	108.570	108.665	109.792	105.057	238.72
3	4	99.02	—	—	182.255	109.292	288.76
2	5	104.95	—	—	226.432	116.385	297.30

$$\delta U_n = \int_{\Omega} \left[ N_x (w_{,x} \delta w_{,x}) + N_{xy} (w_{,x} \delta w_{,y} + \delta w_{,x} w_{,y}) + N_y (w_{,y} \delta w_{,y}) \right] dx dy \quad (19)$$

Here  $w$  denotes the transverse deflection, and  $N_x$ ,  $N_{xy}$ , and  $N_y$  are the stress resultants,

$$N_x = \frac{C_1}{2} (w_{,x}^2 + \nu w_{,y}^2), \quad N_{xy} = C_2 w_{,x} w_{,y}, \quad N_y = \frac{C_1}{2} (w_{,y}^2 + \nu w_{,x}^2) \quad (20)$$

where  $D = Et^3/12(1-\nu^2)$ ,  $C_1 = Et/(1-\nu^2)$ , and  $C_2 = Gt$ ,  $E$  being the Young's modulus,  $G$  the shear modulus,  $\nu$  the Poisson's ratio, and  $t$  the thickness of the plate. Introducing the slopes  $\theta_x$  and  $\theta_y$ ,

$$\frac{\partial w}{\partial x} - \theta_x = 0, \quad \frac{\partial w}{\partial y} - \theta_y = 0 \quad (21)$$

the strain energy in (18) can be written in terms of  $\theta_x$  and  $\theta_y$ ,

$$U_{\theta}(\theta_x, \theta_y) = \frac{D}{2} \int_{\Omega} \left[ \theta_{x,x}^2 + \theta_{y,y}^2 + 2\nu \theta_{x,x} \theta_{y,y} + \frac{(1-\nu)}{2} (\theta_{x,y} + \theta_{y,x})^2 \right] dx dy + U_n(\theta_x, \theta_y) \quad (22)$$

Variation of the functional in (18) leads to the equilibrium equation in terms of the deflection  $w$ , while that of (22) leads to equilibrium equations in terms of the slopes. The strain energy associated with the thick plate (Reissner's) theory is given by

$$U_s = \frac{D}{2} \int_{\Omega} \left[ \psi_{x,x}^2 + \psi_{y,y}^2 + 2\nu \psi_{x,x} \psi_{y,y} + \frac{(1-\nu)}{2} (\psi_{x,y} + \psi_{y,x})^2 \right] dx dy + \frac{ktG}{2} \int_{\Omega} [(w_{,x} - \psi_x)^2 + (w_{,y} - \psi_y)^2] dx dy + U_n(\psi_x, \psi_y) \quad (23)$$

where  $\psi_x$  and  $\psi_y$  are the slope functions and  $k$  is the shear correction factor. Note the similarity of the expressions in (22) and (23).

In the penalty method the problem of finding the critical points  $(\theta_x, \theta_y)$  of the functional  $U_{\theta}$  subject to the constraint conditions (21) is formulated as one of seeking the critical points  $(\theta_x, \theta_y)$  of the modified functional,

$$U_p(\theta_x, \theta_y, w) = U_{\theta}(\theta_x, \theta_y) + \frac{\varepsilon}{2} \int_{\Omega} [(w_{,x} - \theta_x)^2 + (w_{,y} - \theta_y)^2] dx dy \quad (24)$$

without constraints. Here  $\varepsilon$  is the penalty parameter. The penalty parameter  $\varepsilon$  plays a crucial role in the accuracy of the method. In theory, as  $\varepsilon$  goes to infinity, the solution  $(\theta_x(\varepsilon), \theta_y(\varepsilon))$  to the penalty problem approaches the true solution  $(\theta_x, \theta_y)$  (see Reddy [33]). The shear force resultants can be identified as

$$Q_x^{\varepsilon} = \varepsilon \left( \frac{\partial w(\varepsilon)}{\partial x} - \theta_x(\varepsilon) \right), \quad Q_y^{\varepsilon} = \varepsilon \left( \frac{\partial w(\varepsilon)}{\partial y} - \theta_y(\varepsilon) \right) \quad (25)$$

Also note that the penalty functional  $U_p$  is of the same form as the functional  $U_s$  associated with shear flexible theory with the following correspondence:

$$\psi_x \sim \theta_x, \psi_y \sim \theta_y, \epsilon \sim ktG \quad (26)$$

Thus, for a very large value of  $\epsilon$  we recover the strain energy of the thin-plate theory from equation (24), and for  $\epsilon = ktG$ ,  $U_p$  represents the strain energy associated with Reissner's thick-plate theory.

#### 6. PENALTY FINITE-ELEMENT MODEL

The total potential energy associated with the penalty formulation of the equations governing the large deflection of elastic (isotropic) plates is given by

$$\pi_p(w, \theta_x, \theta_y) = U_p(\theta_x, \theta_y, w) - \int_{\Omega} wP \, dx dy - \int_{\partial\Omega_q} \hat{q}w \, ds - \int_{\partial\Omega_m} \hat{M}_n \frac{\partial w}{\partial n} \, ds \quad (27)$$

where  $\partial\Omega_q + \partial\Omega_m = \partial\Omega$ ,  $P$  is the distributed load, and  $n$  is the unit outward normal.

We seek the finite-element solutions of the form

$$w = \sum w_i N_i, \quad \theta_x = \sum \theta_x^i N_i, \quad \theta_y = \sum \theta_y^i N_i \quad (28)$$

where  $N_i$  are the (finite element) shape functions. Substituting (28) into (27), we obtain the following equations for a typical element:

$$\begin{bmatrix} [K^X] + \epsilon[S^0] & [K^{XY}] & -\epsilon[S^{0X}] \\ \text{symmetric} & [K^Y] + \epsilon[S^0] & -\epsilon[S^{0Y}] \\ & & \epsilon[K] \end{bmatrix} \begin{Bmatrix} \{\theta_x\} \\ \{\theta_y\} \\ \{w\} \end{Bmatrix} = \begin{Bmatrix} \{B^X\} \\ \{B^Y\} \\ \{Q\} \end{Bmatrix} \quad (29)$$

where

$$[K^X] = D([S^X] + (1-\nu)[S^Y]) + [G^X], \quad S_{ij}^{\epsilon\eta} = \int_{\Omega} N_{i,\epsilon} N_{j,\eta} d\epsilon d\eta$$

$$[K^Y] = D([S^Y] + (1-\nu)[S^X]) + [G^Y], \quad [K^{XY}] = D[S^{XY}] + [G^{XY}] \quad (30)$$

$$G_{ij}^X = \int_{\Omega} \bar{N}_X N_i N_j dx dy, \quad G_{ij}^Y = \int_{\Omega} \bar{N}_Y N_i N_j dx dy, \quad G_{ij}^{XY} = \int_{\Omega} \bar{N}_{XY} N_i N_j dx dy$$

$$[K] = [S^X] + [S^Y], \quad B_1^X = \int_{\partial\Omega} \hat{M}_X N_1 ds, \quad B_1^Y = \int_{\partial\Omega} \hat{M}_Y N_1 ds$$

Computational Aspects. Several comments are in order on the computational aspects of the penalty finite-element model developed herein. First let us examine the consequence of the limit  $\epsilon^{-1}$  going to zero. The penalty finite-element equation (12) can be expressed in the form

$$([K_1] + \epsilon[K_2])\{\Delta\} = \{F\} \quad (31)$$

For very large values of  $\epsilon$ , the second term (i.e. penalty term) in the parentheses dominates and we have,

$$\frac{1}{\epsilon} \{F\} = \frac{1}{\epsilon} ([K_1] + \epsilon[K_2])\{\Delta\} = [K_2]\{\Delta\}, \quad \text{and} \quad \lim_{\epsilon \rightarrow \infty} [K_2]\{\Delta\} = \{0\} \quad (32)$$

Thus, for a very large value of  $\epsilon$ , the bending-energy contribution to the stiffness matrix is lost (and the energy due to transverse shear dominates), and equation (32) yields, in an attempt to satisfy the constraint conditions exactly, the trivial solution  $\{\Delta\} = \{0\}$  (if  $[K_2]$  is nonsingular). If the equations in (15) are linearly dependent (i.e.  $[K_2]$  is singular), then the number of independent (constraint) equations are less than the number of unknowns and the remaining equations are provided by  $[K_1]$ . Thus, it is necessary to have nonsingular  $[K_1]$  and singular  $[K_2]$  in order to obtain a nontrivial solution. The same conclusion can be reached from a mathematical point of view. The existence and uniqueness of solutions to any finite

element model requires the associated bilinear form to satisfy certain continuity and coercivity conditions (see Oden and Reddy [34]). For the penalty finite-element model, these conditions impose restrictions on the choice of interpolation used for  $w$ , and  $\theta_x$ , and  $\theta_y$  to make the parameter appearing in the coercivity condition be independent of the mesh size,  $h$ . The latter can also be achieved by employing reduced integration on the penalty (or shear) terms, which makes the matrix  $[K_2]$  singular. Reduced integration is employed in the present study to evaluate the elements of  $[K_2]$ . For example, if a bilinear quadrilateral element is used, a 1x1 Gauss rule must be used for  $[K_2]$  in place of the standard 2x2 Gauss rule. As for the value of  $\epsilon$ , it should be equal to  $kGt$  for thick plates (in which  $\theta_x = \psi_x \neq \partial w/\partial x$ , etc.), and an order or two greater for the thin-plate analysis (to satisfy the constraints  $\theta_x = \partial w/\partial x$ , and  $\theta_y = \partial w/\partial y$ ).

#### 7. NONLINEAR BENDING AND FREE VIBRATION RESULTS

The penalty finite element described above is used in the (static) bending analysis of square plates under uniformly distributed load for various edge conditions. In these studies a value of 0.3 is used for the Poisson's ratio, and  $\epsilon$  is taken to be  $Gt/h$ , where  $h$  is the element (mesh) size. Due to the biaxial symmetry of the problems considered here, only quarter plates are analyzed in the interest of computational efficiency and convenience. The following iterative scheme is used to obtain the convergence of the transverse deflections. Beginning with the zero solution, the linear solution is obtained after the first iteration. This solution is used to compute the nonlinear (geometric) stiffness coefficients for the next iteration. Only a weighted average of the following form is used to calculate the geometric stiffness coefficients:

$$\{\Delta\}^{n+1} = \alpha\{\Delta\}^n + (1-\alpha)\{\Delta\}^{n-1} \quad (33)$$

where  $\{\Delta\}$  is the solution vector,  $n$  is the iteration number, and  $\alpha$  is a parameter,  $0 < \alpha < 1$ . Preliminary investigation showed that a value of  $\alpha = 2/3$  gives, in the present formulation, the fastest convergence. The convergence criterion used is of the form,

$$[\sum (\Delta_i^{n+1} - \Delta_i^n)^2]^{1/2} < \epsilon = 10^{-4} \quad (34)$$

All of the computations are carried on an IBM 370/158 model in double precision. Due to the space limitation only limited results are included here.

Figures 3 and 4 show the plots of the (normalized) center deflection for simply-supported and clamped plates, respectively, under uniformly distributed loading, and corresponding stresses are shown in Figures 5 and 6. The present solutions are in good agreement with those of Way [35], Wang [36], Levy [37], and Yamaki [38]. The present solutions (for various meshes and elements) are bounded by Yamaki's solution from above, and Wang's solution from below for simply-supported plate.

Table 9 shows a comparison of the penalty (present) solution with the mixed solution of Reddy and Stricklin [39] for the clamped-hinged square plate under uniformly distributed load. The mixed finite element in [39] was based on the von Karman equations. The bending moments ( $M_x = M_y$ ) are compared, for the same problem, in Table 10. The values of the bending moment are obtained at the nodes in the case of the mixed method, whereas they are computed at the Gaussian points in the case of the penalty method. The locations of the Gaussian points are given in parentheses.

Due to the simplicity of the present element, it is very economical to use in nonlinear problems which require large numbers of elements. The complicated conventional bending elements (i.e. elements based on displacement

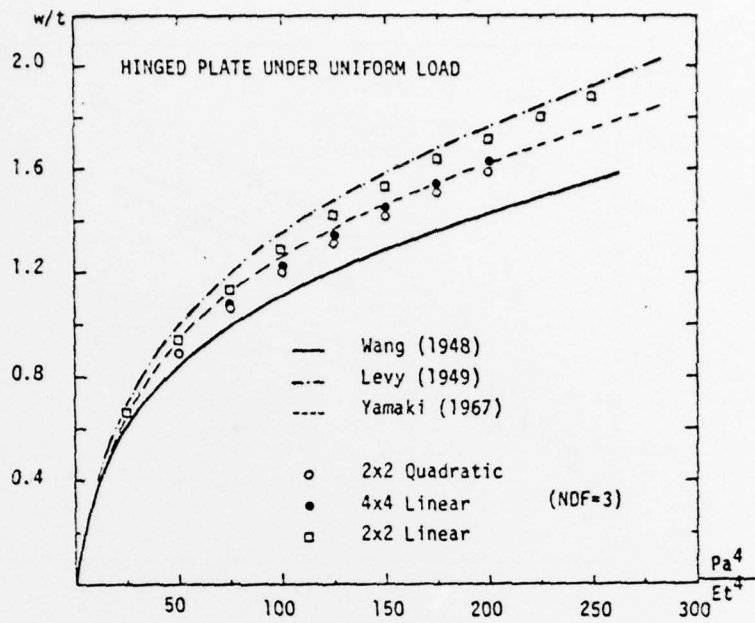


Figure 3 Load-deflection curves for simply supported square plate under uniform loading

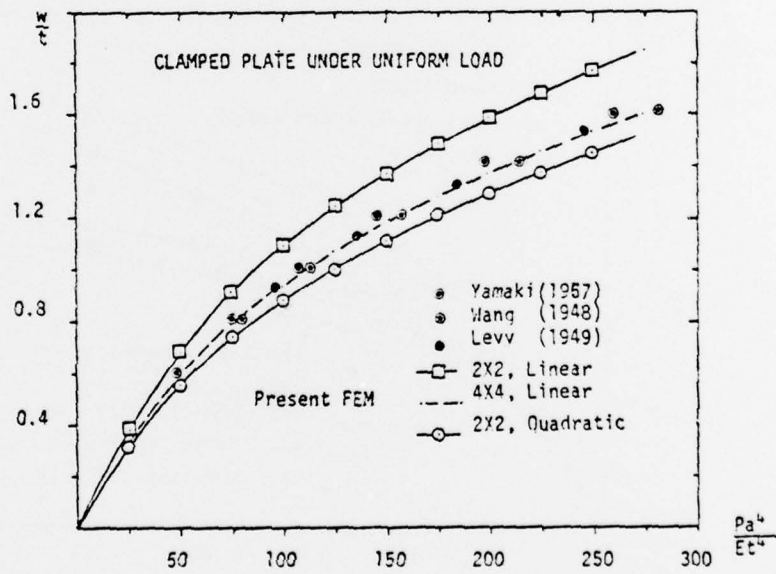


Figure 4 Load-deflection curves for clamped square plate under uniform loading

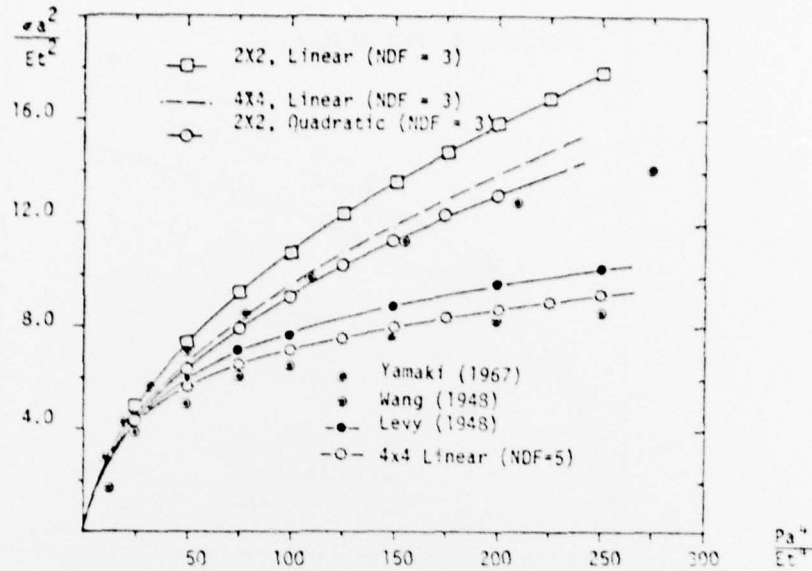


Figure 5 Stress-load curves for simply supported square plate under uniform loading

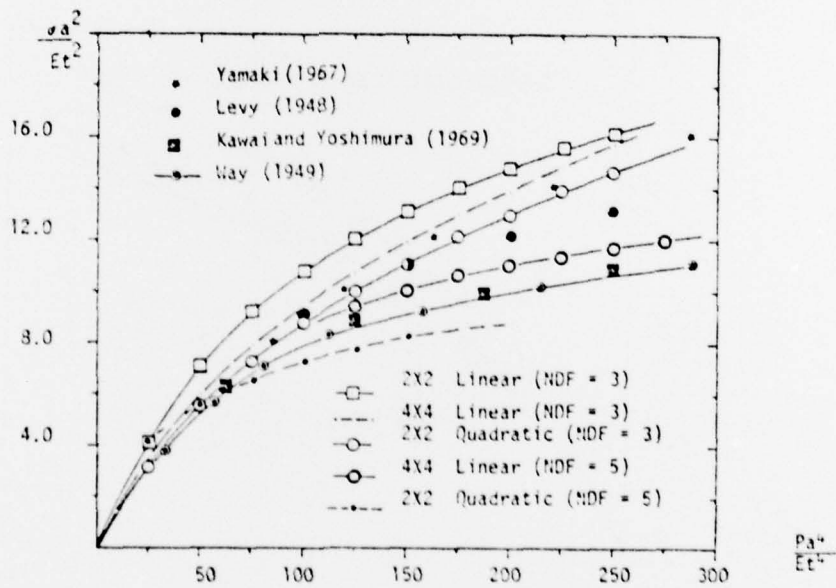


Figure 6 Stress-load curves for clamped square plate under uniform loading

type formulations) are only marginally more accurate when the linear solutions are compared but computationally very expensive.

Table 9. Comparison of Center Deflection ( $w/t$ ) Obtained by the Mixed and Penalty Methods for Clamped-Hinged Square Plate Under Uniformly Distributed Load ( $\nu=0.3$ ,  $a/t = 10$ )

LOAD $Pa^4/Et^4$	MIXED FEM [39]				PENALTY FEM	
	LINEAR		QUADRATIC		LINEAR	QUADRATIC
	2x2	4x4	2x2	4x4	6x6	4x4
25.0	0.494	0.451	0.436	0.437	0.440	0.441
50.0	0.804	0.724	0.697	0.699	0.707	0.707
75.0	1.021	0.916	0.881	0.882	0.895	0.893
100.0	1.190	1.066	1.025	1.026	1.043	1.040
125.0	1.330	1.192	1.146	1.145	1.167	1.163
150.0	1.450	1.301	1.252	1.249	1.275	1.270
175.0	1.557	1.398	1.345	1.341	1.371	1.365
200.0	1.652	1.486	1.431	1.425	1.458	1.452
225.0	1.741	1.566	1.509	1.501	1.539	1.532
250.0	1.821	1.641	1.581	1.572	1.613	---

Table 10. Comparison of Maximum Bending Moment ( $-M_x \times 10^{-2}$ ) Obtained by the Mixed and Penalty Methods for Clamped-Hinged Under Uniformly Distributed Load ( $\nu = 0.3$ ,  $a/t = 10$ )

LOAD $Pa^4/Et^4$	MIXED FEM [39]				PENALTY FEM	
	LINEAR		QUADRATIC		LINEAR	QUADRATIC
	2x2	4x4	2x2	4x4	6x6 (.4583, .4583)	4x4 (.4375, .4375)
25.0	1.450	1.535	1.617	1.572	1.094	0.874
50.0	2.400	2.653	2.829	2.729	1.827	1.420
75.0	3.076	3.558	3.833	3.683	2.381	1.810
100.0	3.616	4.342	4.717	4.527	2.839	2.118
125.0	4.067	5.043	5.518	5.300	3.234	2.375
150.0	4.458	5.683	6.256	6.023	3.585	2.596
175.0	4.806	6.275	6.942	6.707	3.903	2.792
200.0	5.117	6.827	7.590	7.359	4.194	2.967
225.0	5.407	7.346	8.199	7.986	4.464	3.126
250.0	5.671	7.836	8.777	8.592	4.717	-----

## 8. APPLICATION TO PLATES MADE OF BIMODULUS MATERIALS

The finite element model developed herein can also be applied to the analysis of plates constructed of bimodulus composite material. Due to different elastic properties in tension (T) and compression (C), the material coefficients  $A_{ij}$ ,  $B_{ij}$ , and  $D_{ij}$  are now defined by (see [40]),

$$\begin{aligned} (A_{ij}, B_{ij}, D_{ij}) &= \int_{-t/2}^{t/2} Q_{ij} (1, z, z^2) dz, \quad (i, j=1, 2, 6) \\ &= \sum_{\ell=1}^n \int_{z_{\ell}}^{z_n} Q_{ij1\ell} dz + \sum_{\ell=1}^n \int_{z_n}^{z_{\ell+1}} Q_{ij2\ell} dz \end{aligned} \quad (35)$$

Here  $Q_{ijk\ell}$  denote the stiffness coefficients in the plate coordinates of the  $\ell$ -th layer in tension ( $k=1$ ) or compression ( $k=2$ ), and  $z_n$  is the distance from the midsurface to the neutral plane (which is unknown a priori).

Figure 7 shows the influence of the aspect ratio ( $b/a$ ) and side-to-thickness ratio ( $a/t$ ) on the location of neutral surfaces for a single-layer, isotropic, bimodulus, simply supported rectangular plate subjected to sinusoidal loading,

$$p = P_0 \sin(\pi x/a) \sin(\pi y/b)$$

The following elastic properties are used:

$$\begin{aligned} E_{11}^t &= 3.584 \text{ GPa}, \quad E_{11}^c = 1.792 \text{ GPa}, \quad E_{22}^t = E_{11}^t, \quad E_{22}^c = E_{11}^c \\ G_{12}^t &= G_{12}^c = 1.27 \text{ GPa}, \quad \nu_{12}^t = \nu_{21}^t = 0.4, \quad \nu_{12}^c = \nu_{21}^c = 0.2 \end{aligned} \quad (36)$$

Note that for  $b/a = 1$ , the neutral surfaces associated with  $x$ - and  $y$ -directions coincide (i.e.,  $z_{ns} = z_{ny}$ ).

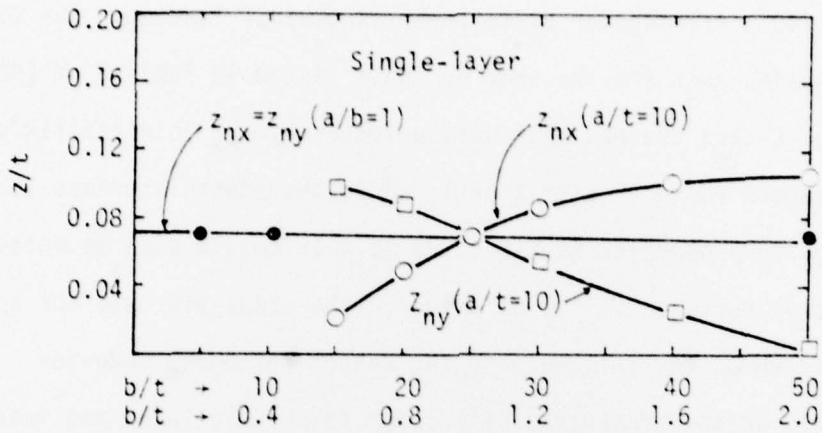


Fig. 7 Neutral-surface location vs. plate aspect ratio, and side-to-thickness ratio for single-layered rectangular plate under sinusoidal loading.

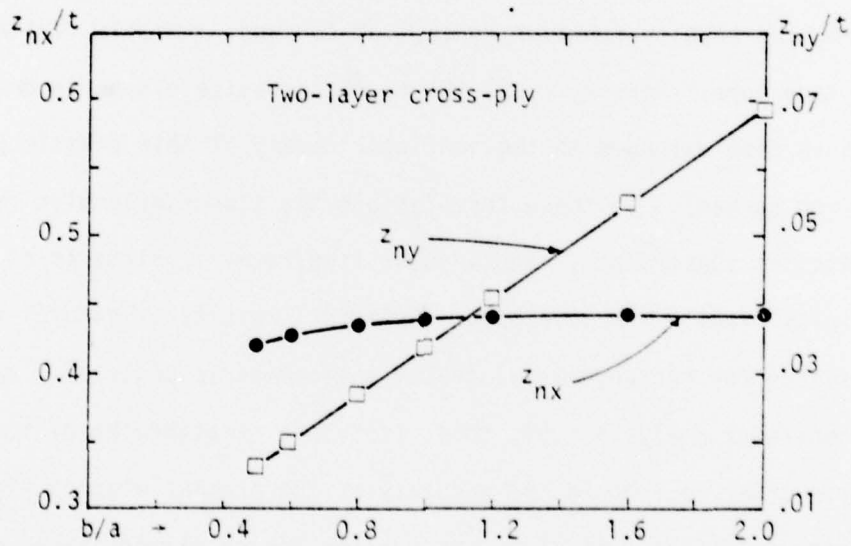


Fig. 8 Neutral-surface location vs. plate aspect ratio for two-layer, cross-ply ( $0^\circ/90^\circ$ ) square plate under sinusoidal loading.

Similar results are presented in Figures 8 and 9 for a two-layer, cross-ply ( $0^\circ/90^\circ$ ) rectangular plate under sinusoidal loading. The bimodulus properties used are the same as those listed in Table 3 of [40]. Note from Fig. 8 that the neutral-surface location,  $z_{nx}$  is virtually unchanged for aspect ratio greater than 1, while the neutral-surface location,  $z_{ny}$ , increases in proportion to aspect ratio. It should also be noted that the neutral surfaces do not coincide in the cross-ply case for  $b/a = 1$ .

Figure 10 shows the influence of the aspect ratio and side-to-thickness ratio on the transverse deflection for single-layer and two-layer cross-ply problems discussed above. The effect of thickness on the deflection is more pronounced than the effect of the aspect ratio.

#### 9. SUMMARY AND CONCLUSIONS

Using the penalty function concept of Courant, a simple finite element for the Yang-Norris-Stavsky (YNS) theory of composite plates is developed. The idea is also extended to the nonlinear theory of thin elastic plates (due to von Karman). In these formulations the slope-deflection relations are treated as constraints. Rectangular isoparametric elements of the "serendipity" family are developed. Numerical results of natural frequencies are presented for rectangular plates of antisymmetric angle-ply laminates. In the nonlinear analysis, only thin, isotropic, rectangular plates are considered in order to compare the accuracy of the present element with other approximate solutions. Finally, the penalty finite element based on the YNS theory is employed to study the bending of laminated, anisotropic bimodulus-material plates.

In the study of free vibrations, the present element gives very accurate results for natural frequencies. The results are verified against closed-

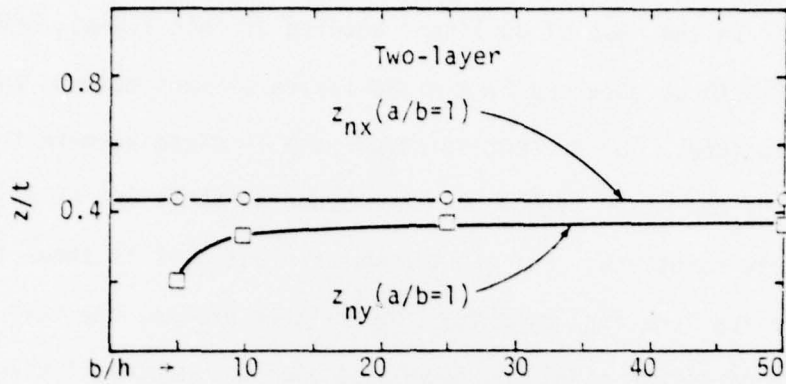


Fig. 9 Neutral-surface location vs. side-to-thickness ratio for two-layer cross-ply ( $0^\circ/90^\circ$ ) rectangular plate under sinusoidal loading.

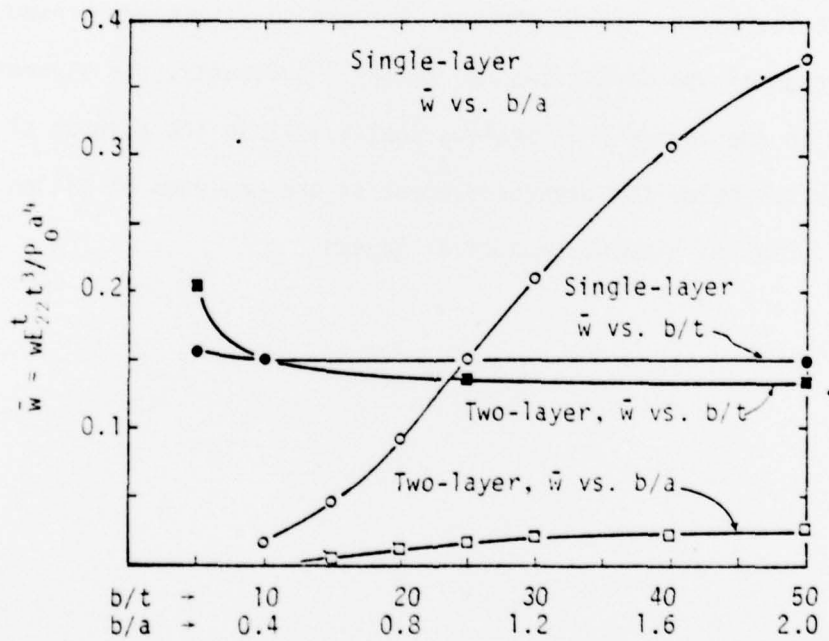


Fig. 10 Transverse deflection vs. plate aspect ratio, and side-to-thickness ratio for single-layer and two-layer cross-ply plates under sinusoidal loading.

form solutions. In the case of nonlinear bending of thin plates, the results are compared with those obtained by a mixed finite element method, and other approximate solutions. The present solutions are in close agreement with those obtained by the mixed method, and are bounded (above and below) by other approximate solutions. For the bimodulus plates, it is shown that the neutral-surface location, even for single-layer plates, may vary considerably from the geometric midplane, depending upon the degree of bimodularity. Also, the plate deflection is significantly affected by the bimodulus action.

The penalty element developed herein is computationally simple and accurate, and saves large amounts of computing time in nonlinear analyses which require iteration. It is straight forward to extend the present element to a combination of von Karman and YNS theory. Obviously, the element can also be used in the analysis of shallow shells. It is the purpose of this investigation to employ the present element in the analyses of plates and shells constructed of bimodulus-material layers.

## REFERENCES

1. R. D. MINDLIN 1951 Journal of Applied Mechanics 18, 31-38, Influence of rotary inertia and shear on flexural motions of isotropic, elastic plates.
2. Y. STAVSKY 1965 Topics in Applied Mechanics, D. Abir, F. Ollendorff, and M. Reiner, eds., American Elsevier, New York, 105, On the theory of symmetrically heterogeneous plates having the same thickness variation of the elastic moduli.
3. P. C. YANG, C. H. NORRIS, and Y. STAVSKY 1966 International Journal of Solids and Structures 2, 665, Elastic wave propagation in heterogeneous plates.
4. C. T. SUN and J. M. WHITNEY 1973 American Institute of Aeronautics and Astronautics Journal 11, 178, Theories for the dynamic response of laminated plates.
5. J. M. WHITNEY and C. T. SUN 1973 Journal of Sound and Vibration 30, 85, A higher order theory for extensional motion of laminated composites.
6. C. W. BERT 1974 Structural Design and Analysis, Part I, C. C. Chamis, ed., Academic Press, New York, Ch. 4, Analysis of plates.
7. S. SRINIVAS and A. K. RAO 1970 International Journal of Solids and Structures 6, 1463-1481, Bending, vibration and buckling of simply supported thick orthotropic rectangular plates and laminates.
8. S. SRINIVAS, C. V. JOGA RAO, and A. K. RAO 1970 Journal of Sound and Vibration 12(2), 187-199, An exact analysis for vibration of simply supported homogeneous and laminated thick rectangular plates.
9. J. M. WHITNEY and N. J. PAGANO 1970 Journal of Applied Mechanics 37, 1031, Shear deformation in heterogeneous anisotropic plates.
10. R. C. FORTIER and J. N. ROSSETTOS 1973 Journal of Applied Mechanics 40, 299, On the vibration of shear deformable curved anisotropic composite plates.
11. P. K. SINHA and A. K. RATH 1975 Aeronautical Quarterly 26, 211, Vibration and buckling of cross-ply laminated circular cylindrical panels.
12. C. W. BERT and T. L. C. CHEN 1978 International Journal of Solids and Structures 14, 6, 465-473, Effect of shear deformation on vibration of antisymmetric angle-ply laminated rectangular plates.
13. A. K. NOOR and M. D. MATHERS 1976 American Institute of Aeronautics and Astronautics Journal 14, 282-285, Anisotropy and shear deformation in laminated composite plates.

14. A. K. NOOR and M. D. MATHERS 1977 International Journal for Numerical Methods in Engineering 11, 289-307, Finite element analysis of anisotropic plates.
15. E. HINTON 1976 Earthquake Engineering and Structural Dynamics 4, 511-514, A note on a thick finite strip method for the free vibration of laminated plates (short communication).
16. E. HINTON 1976 Earthquake Engineering and Structural Dynamics 4, 515-516, A note on a finite element method for the free vibrations of laminated plates (short communication).
17. R. M. JONES 1975 Mechanics of Composite Materials, New York: McGraw-Hill Book Company, Inc.
18. R. D. MINDLIN, A. SCHACKNOW, and H. DERESIEWICZ 1956 Journal of Applied Mechanics 23, 431, Flexural vibrations of rectangular plates.
19. T. A. ROCK and E. HINTON 1976 Computers and Structures 6, 37-44, A finite element method for the free vibration of plates allowing for transverse shear deformation.
20. R. M. JONES, H. S. MORGAN, and J. M. WHITNEY 1973 Journal of Applied Mechanics 40, 1143, Buckling and vibration of antisymmetrically laminated angle-ply rectangular plates.
21. J. N. REDDY 1979 A simple plate bending element for the analysis of laminated anisotropic composite plates, in review.
22. T. KAWAI and N. YOSHIMURA 1969 International Journal for Numerical Methods in Engineering 1, 123-133, Analysis of large deflection of plates by the finite element method.
23. L. R. HERRMANN 1967 Journal of Engineering Mechanics Division, ASCE 93, EM5, 13-26, Finite element bending analysis for plates.
24. S. NASSER-NEMAT and K. N. LEE 1973 Developments in Mechanics 7, (Proc. of the 13th Midwestern Mechanics Conference), 979-995, Finite element formulations for elastic plates by general variational statements and discontinuous fields.
25. F. KIKUCHI and Y. ANDO 1973 Nuclear Engineering and Design 24, 357-373, On the convergence of a mixed finite element scheme for plate bending.
26. J. N. REDDY and C. S. TSAY 1977 Journal of Sound and Vibration 55, 2, 289-302, Stability and vibration of thin rectangular plates by simplified mixed finite elements.

27. G. WEMPNER, J. T. ODEN, and D. KROSS 1968 Journal of Engineering Mechanics Division, Proceedings ASCE 94, 1273-1294, Finite element analysis of thin shells.
28. I. FRIED 1973 International Journal of Solids and Structures 9, 449-460, Shear in  $C^0$  and  $C^1$  plate bending elements.
29. I. FRIED 1974 Computers and Structures 4, 771-778, Residual energy balancing technique in the generation of plate bending finite elements.
30. O. C. ZIENKIEWICZ and E. HINTON 1976 Journal of the Franklin Institute 302, 443-361, Reduced integration, function smoothing and non-conformity in finite element analysis.
31. T. J. R. HUGHES, M. COHEN, and M. HAROUN 1978 Nuclear Engineering and Design 46, 1, 203-222, Reduced and selective integration techniques in the finite element analysis of plates.
32. R. COURANT 1956 Calculus of Variations and Supplementary Notes and Exercises, Revised and Amended by J. Moser, New York: New York University.
33. J. N. REDDY 1978 International Journal of Engineering Science 16, 12, 921-929, On the accuracy and existence of solutions to the primitive variable models of viscous incompressible fluids.
34. J. T. ODEN and J. N. REDDY 1976 An Introduction to the Mathematical Theory of Finite Elements, New York: Wiley-Interscience.
35. C. T. WANG 1948 NACA 1462, Bending of rectangular plates with large deflections.
36. S. LEVY 1942 \*NACA 737, Bending of rectangular plates with large deflections.
37. N. YAMAKI 1967 ZAMM 41, 501-510, Influence of large amplitudes on flexural vibrations of elastic plates.
38. S. WAY 1939 Proceedings of 5th International Congress in Applied Mechanics, 123-128, Uniformly loaded, clamped, rectangular plates with large deformation.
39. J. N. REDDY and J. D. STRICKLIN 1976 Applications of Computer Methods in Engineering II, 1323-1335, Wellford, Jr. L.C. (ed.), Los Angeles: University of Southern California, Large deflection and large amplitude free vibrations of thin rectangular plates using mixed isoparametric elements.
40. J. N. REDDY and C. W. BERT 1979 Mechanics of Bimodulus Materials, C. W. Bert (ed.), ASME Winter Annual Meeting, New York, Analysis of plates constructed of fiber-reinforced bimodulus materials, to appear.

UNCLASSIFIED

SECURITY CLASSIFICATION OF THIS PAGE (When Data Entered)

REPORT DOCUMENTATION PAGE		READ INSTRUCTIONS BEFORE COMPLETING FORM
1. REPORT NUMBER <b>14</b> OU-AMNE-79-9, TR-3	2. GOVT ACCESSION NO.	3. RECIPIENT'S CATALOG NUMBER
4. TITLE (and Subtitle) <b>6</b> FINITE-ELEMENT ANALYSIS OF Laminated COMPOSITE-MATERIAL PLATES	5. TYPE OF REPORT & PERIOD COVERED Technical Report, No. 3	
7. AUTHOR(s) <b>10</b> J. N./Reddy	8. CONTRACT OR GRANT NUMBER(s) <b>15</b> N00014-78-C-0647	
9. PERFORMING ORGANIZATION NAME AND ADDRESS School of Aerospace, Mechanical and Nuclear Engineering University of Oklahoma, Norman, OK 73019	10. PROGRAM ELEMENT, PROJECT, TASK AREA & WORK UNIT NUMBERS NR 064-609	
11. CONTROLLING OFFICE NAME AND ADDRESS Department of the Navy, Office of Naval Research Structural Mechanics Program (Code 474) Arlington, Virginia 22217	12. REPORT DATE June 1979	
14. MONITORING AGENCY NAME & ADDRESS (if different from Controlling Office) <b>12</b> 48 P.	13. NUMBER OF PAGES 37	
16. DISTRIBUTION STATEMENT (of this Report)  This document has been approved for public release and sale; distribution unlimited.	15. SECURITY CLASS. (of this report) UNCLASSIFIED	
17. DISTRIBUTION STATEMENT (of the abstract entered in Block 20, if different from Report)	15a. DECLASSIFICATION/DOWNGRADING SCHEDULE	
13. SUPPLEMENTARY NOTES Portion of the report on the free vibrations of antisymmetric angle-ply laminated plates is to appear in the Journal of Sound and Vibration, and the portion on the nonlinear bending of thin isotropic plates will (over)		
19. KEY WORDS (Continue on reverse side if necessary and identify by block number) Bimodulus materials, fiber-reinforced composites, finite elements, laminated plates, mixed finite element method, natural frequencies, penalty method, shear flexible plate theory, variational formulations, von Karman nonlinear plate theory.		
20. ABSTRACT (Continue on reverse side if necessary and identify by block number) A finite-element formulation of the equations governing the laminated anisotropic plate theory of Yang, Norris and Stavsky, is presented. The theory is a generalization of Mindlin's theory for isotropic plates to laminated anisotropic plates and includes shear deformation and rotary inertia effects. Finite-element solutions are presented for rectangular plates of antisymmetric angle-ply laminates having material properties that are typical of a highly anisotropic composite material. Two sets of (over) →		

DD FORM 1 JAN 73 1473

EDITION OF 1 NOV 65 IS OBSOLETE  
S/N 0102-014-6601

UNCLASSIFIED

SECURITY CLASSIFICATION OF THIS PAGE (When Data Entered)

400 498

elt

UNCLASSIFIED

SECURITY CLASSIFICATION OF THIS PAGE (When Data Entered)

20. ABSTRACT (cont'd)

material properties that are typical of advanced fiber-reinforced composites are used to show the parametric effects of plate aspect ratio, length-to-thickness ratio, number of layers, and lamination angle. The element is also employed to study the bending of laminated, anisotropic bimodulus material-plates. Results are presented for single-layer and two-layer cross-ply rectangular plates subjected to sinusoidal loading.

The report also presents a  $C^0$  finite element for the von Karman equations of thin elastic plates. The slope-displacement relations are treated as constraints using the so-called penalty method of Courant. The resulting element contains the transverse deflection and two slopes as nodal degrees of freedom. By selecting an appropriate value of the penalty parameter, solutions for thin as well as thick plates are obtained. Numerical results are presented for rectangular plates with various edge conditions.

18. Supplementary Notes (cont'd)

appear in the Proceedings of the Third International Conference in Australia on Finite Element Methods, Sydney, Australia, 1979.

UNCLASSIFIED

SECURITY CLASSIFICATION OF THIS PAGE (When Data Entered)